Multiple magnetization steps and plateaus across the antiferromagnetic to ferromagnetic transition in $La_{1-x}Ce_xFe_{12}B_6$: Time delay of the metamagnetic transitions

L. V. B. Diop* and O. Isnard
Université Grenoble Alpes, CNRS, Institut Néel, 38000 Grenoble, France

(Received 7 November 2017; revised manuscript received 2 January 2018; published 29 January 2018)

The effects of cerium substitution on the structural and magnetic properties of the $La_{1-x}Ce_xFe_{12}B_6$ ($0 \leqslant x \leqslant 0.175$) series of compounds have been studied. All of the compounds exhibit an antiferromagnetic ground state below the Néel temperature $T_N \approx 36$ K. Both antiferromagnetic and paramagnetic states can be transformed into the ferromagnetic state irreversibly and reversibly depending on the magnitude of the applied magnetic field, the temperature, and the direction of their changes. Of particular interest is the low-temperature magnetization process. This process is discontinuous and evolves unexpected huge metamagnetic transitions consisting of a succession of sharp magnetization steps separated by plateaus, giving rise to an unusual avalanchelike behavior. At constant temperature and magnetic field, the evolution with time of the magnetization displays a spectacular spontaneous jump after a long incubation time. $La_{1-x}Ce_xFe_{12}B_6$ compounds exhibit a unique combination of exceptional features like large thermal hysteresis, giant magnetization jumps, and remarkably huge magnetic hysteresis for the field-induced first-order metamagnetic transition.

DOI: 10.1103/PhysRevB.97.014436

I. INTRODUCTION

Metamagnets with a first-order phase transition from a low magnetic moment state to a high magnetic moment state have attracted much attention these last years [1–11]. Metamagnetic transition is observed for a variety of metallic and nonmetallic systems and belongs to one of the most interesting magnetic phenomena [12,13]. The most fascinating systems are those where the magnetic-field-induced phase transition is coupled with a change in the crystal structure giving rise to many interesting physical properties. The discovery of giant magnetocaloric effect in magnetic materials exhibiting a metamagnetic transition such as $Gd_5Si_2Ge_2$ [14] and $La(Fe,Si)_{13}$ [15], has opened new perspectives for magnetic refrigeration (a solid-state cooling method). This has triggered the development of many studies from the technological side as well as from the fundamental physics point of view. Magnetic cooling may be a promising alternative to conventional gas compression-expansion refrigeration due to its high energy efficiency and minimal environmental impact. Profoundly important to fundamental research and the application of magnetic cooling is the need to understand how the metamagnetic phase transition evolves, and whether it can be manipulated by chemical substitutions to be sharper, or to occur at a lower magnetic driving field or with minimum hysteresis.

Recently, peculiar metamagnetic transitions between the antiferromagnetic (AFM) and the ferromagnetic (FM) states have been reported in phase-separated manganese oxides. The first magnetization curves recorded at very low temperatures (typically below 5 K) display unusual steplike field dependence [7,8,16–23]. The sharp steps are not only seen in the magnetization isotherms but have also been observed in the magnetic-field dependence of the electrical resistivity and the heat capacity. These intriguing steps are an *intrinsic* feature of the phase-separated manganites independent of the material form (i.e., polycrystalline, single crystalline, or epitaxial film form). The position and number of jumps depend on the magnetic and thermal history of the sample and on the magnetic-field sweep rate. That is, the expression of the *intrinsic* behavior of the phase-separated manganites can be strongly affected by *extrinsic* measurement protocols. Most recently, field-induced steplike transitions have been reported for the highly insulating metal oxide $Er_2Cu_2O_5$ [24]. Among the intermetallics, this kind of staircaselike behavior is rare. Steplike metamagnetic transitions have scarcely been observed in few rare-earth-based intermetallic compounds like Gd_5Ge_4 [8,25–30], Nd_5Ge_3 [31], and doped $CeFe_2$ [32–34]. This unusual step behavior across the magnetic-field-induced AFM-FM phase transition seen in a number of oxides and few intermetallics is attracting an increasing interest. Although belonging to different classes of materials, these oxides and intermetallics present the common features of phase coexistence and strong magnetostructural coupling associated with the first-order AFM-FM transition. Interestingly, multistep metamagnetic transitions in $LaFe_{12}B_6$, a purely 3*d* itinerant-electron system, were recently discussed [35–39].

The ternary system $RT_{12}B_6$ (where R stands for a rare-earth element or yttrium and T is one of the late 3*d* transition elements Fe and Co) adopts the rhombohedral $SrNi_{12}B_6$-type structure, space group $R\bar{3}m$ [40–42]. The 3*d* atoms are located on two inequivalent crystal sites (18*g* and 18*h*) with the rare-earth and boron atoms occupying the 3*a* and 18*h* positions, respectively. The $RCo_{12}B_6$ compounds are stable for essentially all of the rare-earths (except europium) with unit-cell parameters that follow the conventional lanthanide contraction [43]. While $NdFe_{12}B_6$ was the first iron-based

*Present adress: Institut für Materialwissenschaft, Technische Universität Darmstadt, D-64287 Darmstadt, Germany.

examples of the $RT_{12}B_6$ series of compounds to be discovered [44], it is, however, metastable and $LaFe_{12}B_6$ is the only stable Fe-based member of the 1:12:6 family [45,46]. $LaFe_{12}B_6$ is unique among the $RT_{12}B_6$ compounds in being an antiferromagnet. $LaFe_{12}B_6$ also exhibits unique magnetic behavior including an unusual amplitude-modulated spin arrangement, particularly small Fe moment in the ground state, a multicritical point in the magnetic phase diagram, both conventional and inverse magnetocaloric effects, and remarkably low Néel temperature $T_N = 36$ K [35,47]. Neutron powder diffraction studies on $LaFe_{12}B_6$ revealed that the amplitude-modulated antiferromagnetic structure can be described with a magnetic propagation vector of $(\frac{1}{4}, \frac{1}{4}, \frac{1}{4})$ at 1.5 K and in zero field. The Fe magnetic moments are confined to the basal plane with a maximum value of 0.43 μ_B [35] that is remarkably reduced in comparison with the elemental Fe magnetic moment of 2.2 μ_B. The ordering temperature of $LaFe_{12}B_6$ is an order of magnitude smaller than the ordering temperature of any iron-rich R-Fe binary system and in any case much smaller compared to the ferro- (R = Y, La–Sm) or ferri- (R = Gd−Tm) magnets ($T_C = 134-162$ K) [43]. ^{57}Fe Mössbauer spectroscopy and high magnetic field (up to 35 T) studies on pseudoternary compounds of $LaFe_{12-x}Co_xB_6$ [45] and $La_{1-x}Gd_xFe_{12}B_6$ [46] have demonstrated that $LaFe_{12}B_6$ is a compound with Fe moments close to magnetic instability. This unstable character of the Fe moment has been confirmed by tight-binding calculations which further pointed out that the magnetic moment of Fe on the 18h site is more sensitive to its chemical environment [48,49].

In this paper, we present a detailed experimental study of the effects of cerium substitution on the structural and magnetic properties of the $La_{1-x}Ce_xFe_{12}B_6$ ($0 \leqslant x \leqslant 0.175$) series of compounds revealing sharp metamagnetic transitions. The critical magnetic fields of the multiple step transitions were found to be extremely sensitive to cerium doping. We have demonstrated that giant spontaneous magnetization steps occur in relaxation experiments when both the temperature and magnetic field are constant.

II. METHODS

Polycrystalline alloys of $La_{1-x}Ce_xFe_{12}B_6$ ($0 \leqslant x \leqslant 0.175$) have been synthetized by arc melting high-purity starting elements (Alfa Aesar, La—99.9%, Ce—99.9%, Fe—99.99%, B—99.9%) under a purified argon gas atmosphere. To promote homogeneity, the alloys were remelted several times. Small pieces of the ingots were wrapped in tantalum foil, sealed in evacuated quartz tubes, and subsequently annealed at 900 °C for 3 weeks. The synthesized materials were characterized by chemical analysis, as well as by standard x-ray diffractometry. X-ray powder diffraction was performed on a Siemens D5000 diffractometer in reflection mode with the Bragg-Brentano geometry, using Co $K\alpha$ radiation, with a scan step of 0.02° and an angular 2θ range from 20° to 90°. A precise determination of the unit-cell parameters was obtained by a least-squares refinement of the diffraction patterns, including all the observed Bragg reflections. Following the x-ray diffraction analysis, magnetic susceptibility and magnetization measurements were carried out. The magnetic measurements were undertaken on powder samples over a wide temperature range from 1.7 to 300 K. The measurements employed the extraction method in an experimental setup that has been described elsewhere [50]. Temperature, field, and time dependences of the magnetization were measured in steady magnetic fields up to 10.5 T. The ac magnetic susceptibility was measured at a frequency of 10 kHz down to 4.2 K in a magnetic field of 3 mT.

TABLE I. Lattice parameters and unit-cell volume for the $La_{1-x}Ce_xFe_{12}B_6$ series of compounds obtained from x-ray diffraction at room temperature.

x	a (Å)	c (Å)	V (Å^3)
0	9.631(2)	7.612(1)	611.43(09)
0.05	9.630(2)	7.612(1)	611.35(11)
0.1	9.630(3)	7.610(1)	611.09(13)
0.15	9.629(2)	7.607(1)	610.87(12)
0.175	9.629(3)	7.606(1)	610.73(08)

All the magnetization data in the present work were corrected for the presence of the minor Fe_2B impurity phase to get the intrinsic magnetic properties of the $La_{1-x}Ce_xFe_{12}B_6$ series of compounds. Two different methods were employed to determine the amount of impurity: x-ray diffraction analysis and magnetic measurements. The latter measurements were realized just above the ordering temperatures of $La_{1-x}Ce_xFe_{12}B_6$ in order to remain far below the Curie point of Fe_2B, which is 1015 K. The traces of Fe_2B impurity were consequently considered as carrying a saturated magnetic moment simplifying the correction for its ferromagnetic contribution.

III. RESULTS AND DISCUSSION

A. Structural properties

Microprobe analysis performed on the as-cast and annealed samples reveals their high chemical purity. The samples contain a major phase $La_{1-x}Ce_xFe_{12}B_6$ with some amount of the binary system Fe_2B. In order to minimize the quantity of this secondary phase, the nominal compositions were adjusted, after which the $La_{1-x}Ce_xFe_{12}B_6$ intermetallic compounds were found to be mainly single phase according to the analysis of the x-ray diffraction patterns. The analysis of the diffractograms confirms that the $R\bar{3}m$ space group symmetry is retained for all the investigated compounds. A careful look at the diffraction patterns indicates the presence of residual traces of the binary Fe_2B impurity. The unit-cell parameters of the rhombohedral $LaFe_{12}B_6$ compound at room temperature are $a = 9.631$ Å and $c = 7.612$ Å, which are in good agreement with earlier studies [45]. The lattice parameters for the entire series of samples are summarized in Table I, confirming the presence of a solid solution over the entire composition range studied. Within experimental error, unit-cell parameters of $La_{1-x}Ce_xFe_{12}B_6$ compounds slightly decrease with the Ce content. Such a change in unit-cell parameters is due to the smaller atomic size of Ce atoms compared to that of La atoms. Hence the substitution of Ce for La in these intermetallic compounds produces the effect of "chemical pressure" on the crystal lattice. Samples with higher cerium contents ($x = 0.2$, 0.25, and 0.3) were synthesized; however, they were found to contain much

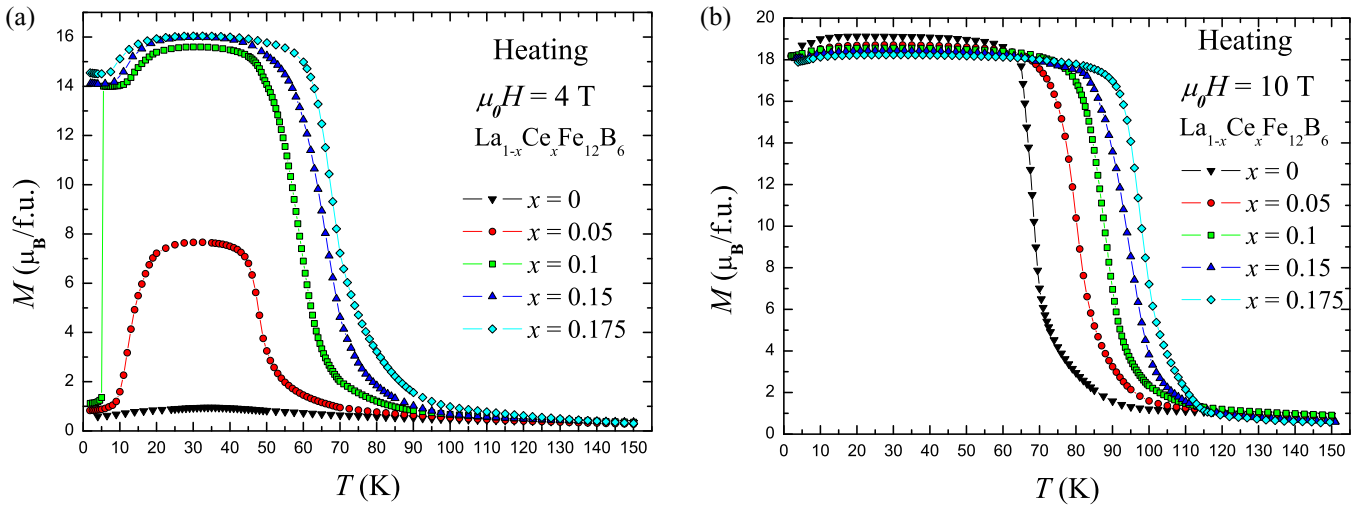

FIG. 1. Temperature dependence of the magnetization of ZFC $La_{1-x}Ce_xFe_{12}B_6$ measured on heating in applied magnetic field of (a) 4 T, and (b) 10 T.

larger amounts of the extra phase. Therefore, those samples with $x \geqslant 0.2$ were not considered further in the present study.

B. Thermal dependence of the magnetization: Zero-field-cooled and field-cooled cooling $M(T)$ data

The low-field temperature dependencies of the magnetization of $La_{1-x}Ce_xFe_{12}B_6$ alloys studied so far exhibit a similar anomaly around 36 K, which is practically independent of the alloy composition and reflects the transition from an AFM to a paramagnetic (PM) state. This ordering temperature is remarkably low and unusual for iron-rich compounds. Figure 1(a) illustrates temperature dependencies of the magnetization of zero-field-cooled (ZFC) samples measured on heating in a 4 T magnetic field. The magnetization of the parent compound $LaFe_{12}B_6$ has only a small broad maximum of 0.95 μ_B/f.u., at 36 K, while the magnetization of $La_{0.95}Ce_{0.05}Fe_{12}B_6$ exhibits a plateaulike anomaly, 7.70 μ_B/f.u. This belllike behavior correlates with the presence of both the low-temperature AFM-FM and high-temperature FM-PM transformations in the sample, and indicates that the FM state in the ZFC $La_{0.95}Ce_{0.05}Fe_{12}B_6$ exists only in a narrow temperature interval in the 4 T magnetic field. Even more intriguing is the thermomagnetic curve for $La_{0.9}Ce_{0.1}Fe_{12}B_6$: On heating from 2 K the magnetization displays a tremendous change from ~1 to ~14 μ_B/f.u. when the temperature increases only by 0.5 K. The sharp magnetization step on the low-temperature part is followed by a gradual growth plus a plateau, while the high-temperature FM-PM transition remains continuous. This abrupt change in magnetization reflects a transition induced by temperature variation in the 4 T applied field. The magnetization shown in Fig. 1(a) indicates that in a 4 T magnetic field, a large fraction, ~80%, of the $La_{0.825}Ce_{0.175}Fe_{12}B_6$ sample is in the ferromagnetic state while $LaFe_{12}B_6$ is completely antiferromagnetic. Figure 1(b) shows ZFC $M(T)$ measurements conducted in a 10 T magnetic field; all samples have a fully ferromagnetic state. The FM-PM transition temperature measured on heating increases nearly linearly with the Ce content at a rate of ~32 K/at. % Ce.

In order to illustrate the gradual change in $M(T)$ in various magnetic fields and the underlying magnetic phase transitions, we present in Fig. 2 both the ZFC and field-cooled cooling (FCC) data of $La_{0.85}Ce_{0.15}Fe_{12}B_6$. On heating in magnetic fields ($\mu_0 H = 1$ and 2.5 T), the magnetization of the ZFC $La_{0.85}Ce_{0.15}Fe_{12}B_6$ exhibits successive magnetic transitions from AFM to PM via a FM state. The observed belllike anomaly is centered at ~34 K, and both its magnitude and width increase with the applied magnetic field. In magnetic fields exceeding ~6.5 T at 2 K, $La_{0.85}Ce_{0.15}Fe_{12}B_6$ is already transformed into a FM state. Hence the temperature dependence of the magnetization reflects only the FM-PM phase transition. On cooling, the magnetization of $La_{0.85}Ce_{0.15}Fe_{12}B_6$ changes similarly to that observed on heating in applied fields exceeding 6.5 T, and displays a huge thermal hysteresis of ~12 K in the vicinity of the FM-PM transformation. This thermal hysteresis is one of the classical intrinsic features of a first-order phase transition. When cooled in magnetic

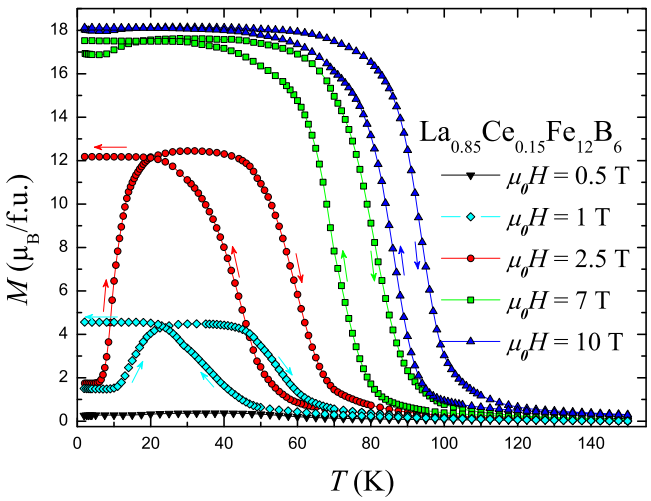

FIG. 2. Temperature dependence of the magnetization of ZFC $La_{0.85}Ce_{0.15}Fe_{12}B_6$ measured in applied magnetic fields of 0.5, 2.5, 7, and 10 T (both ZFC and FC measurements are marked by the same symbols. The direction of the temperature change is indicated by arrows).

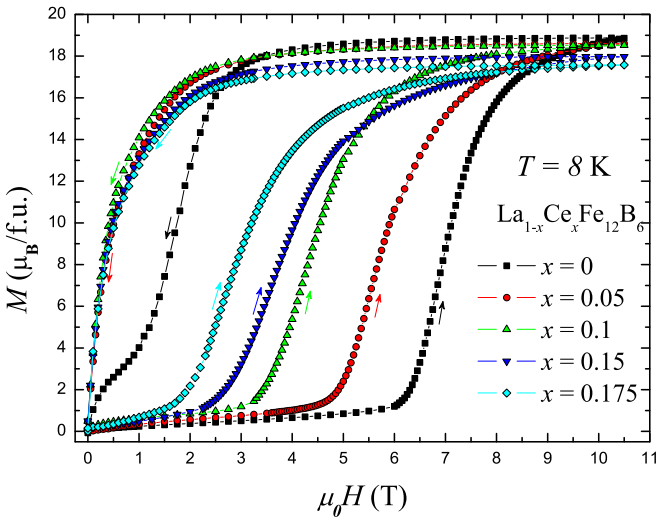

FIG. 3. Isothermal magnetization of $La_{1-x}Ce_xFe_{12}B_6$ series of compounds measured at 8 K.

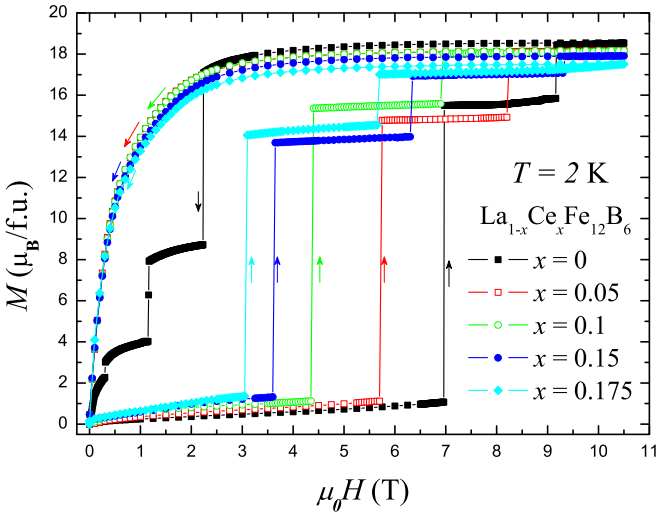

FIG. 4. Isothermal magnetization of $La_{1-x}Ce_xFe_{12}B_6$ series of compounds measured at 2 K.

fields ($\mu_0 H = 1$ and 2.5 T), $La_{0.85}Ce_{0.15}Fe_{12}B_6$ transforms only partially into the FM state. One can also remark that the maximum value of the 2.5 T thermomagnetic curve is larger for the ZFC data than for the FCC data, which is quite unusual for standard ferromagnets.

By comparison to Ref. [35], it appears from Fig. 1 that the effect of Ce substitution is similar to the application of additional magnetic field in the undoped compound $LaFe_{12}B_6$. The ZFC curve in 4 T for $La_{0.95}Ce_{0.05}Fe_{12}B_6$ is similar to the isofield thermomagnetic curves obtained in magnetic fields $\mu_0 H = 5$, 5.5, and 6 T for the parent undoped compound. The $M(T)$ measurement of $LaFe_{12}B_6$ performed in 7 T presents a sudden jump in the low-temperature part. It is quite intriguing that such discontinuity is observed for the magnetization of $La_{0.9}Ce_{0.1}Fe_{12}B_6$ measured in 4 T. Hence a similar temperature dependence of Fe magnetic moment behavior in $La_{1-x}Ce_xFe_{12}B_6$ compounds can be determined by a composition or by a magnetic field. As mentioned above, the Néel temperature T_N is practically independent of the alloy composition, while the FM-PM transition temperature T_C increases with the Ce content at a rate of ~32 K/at. % Ce. Also, T_C of the $LaFe_{12}B_6$ compound increases with magnetic field at a rate of 5.7 K/T. In contrast to the strong effect of an applied magnetic field on T_C, the Néel temperature of $LaFe_{12}B_6$ is barely sensitive to the external magnetic field. Our data show a similar influence of the composition and magnetic field on the development and stability of ferromagnetically and antiferromagnetically ordered phases in $La_{1-x}Ce_xFe_{12}B_6$ alloys. A comparison of these parameters indicates that the substitution of 0.35 at. % of Ce for La is equivalent to an applied magnetic field of 2 T.

C. Isothermal magnetization behavior $M(\mu_0 H)$

In Fig. 3 we compare the isothermal magnetization $M(\mu_0 H)$ at 8 K of the thermally demagnetized $La_{1-x}Ce_xFe_{12}B_6$ ($0 \leqslant x \leqslant 0.175$). The magnetization isotherms exhibit a magnetic-field-induced metamagnetic phase transition between the AFM and FM states. The metamagnetic transition is remarkable by the huge magnetization change but also by the presence of an unusually large magnetic hysteresis. The hysteresis for the field-induced AFM-FM phase transition becomes smaller with increasing Ce content. The observed hysteresis in the magnetization process upon increasing and decreasing fields confirms the first-order nature of the AFM-FM magnetic transition. Figure 3 shows clearly a large sensitivity of the field-induced transformation to the chemical composition; one can notice a strong shift of the metamagnetic transition to lower magnetic fields upon increasing Ce content. This indicates that even a very small substitution of Ce atoms for La atoms strongly affects magnetic correlations between Fe atoms.

Isothermal magnetization of the ZFC $La_{1-x}Ce_xFe_{12}B_6$ has been measured at temperatures well below 8 K. The virgin curves at very low temperatures display more peculiar magnetization process and provide useful information for the interpretation of the magnetization jump observed in the 4 T thermomagnetic curve of $La_{0.9}Ce_{0.1}Fe_{12}B_6$. With lowering of the temperature, the nature of the magnetization isotherms changes dramatically. Field-dependent magnetization curves at 2 K for the $La_{1-x}Ce_xFe_{12}B_6$ series of compounds are depicted in Fig. 4. For the first magnetization curves, a linear behavior typical of an antiferromagnetic state is observed for low external fields ($\mu_0 H < \mu_0 H_{cr1}$). Furthermore, the total magnetic moment changes in a series of large discrete jumps followed by plateaus giving rise to a staircaselike magnetization process. At 2 K, the metamagnetic phase transition between the AFM ground state and the field-driven FM state occurs via magnetic avalanches. The "ultrasharp and multistep" behavior across the AFM-FM transition can be understood if one assumes that at 2 K only a fraction of the specimen volume gets converted into a FM state during the first step. The remaining fraction turns only at higher magnetic transition fields. The saturation value (final magnetization recorded at 10.5 T) corresponds to the case of having the whole sample in the FM state. The saturation moment decreases from 18.55 μ_B/f.u. for $x = 0$ to 17.50 μ_B/f.u. for $x = 0.175$. It is immediately apparent from a visual inspection of the field-decreasing leg that there

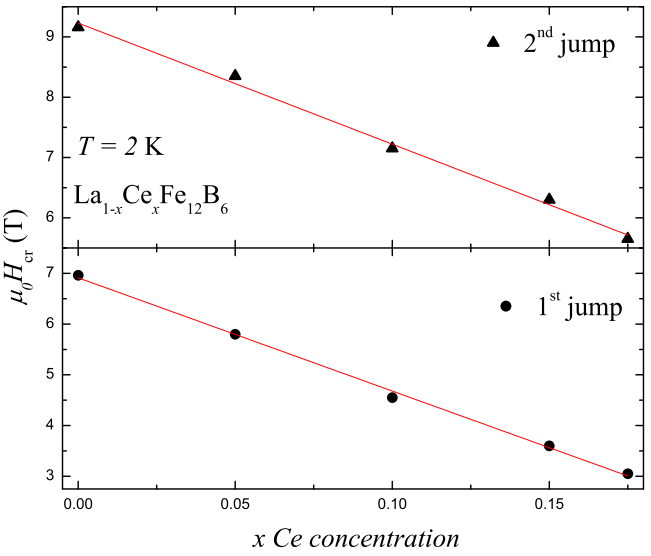

FIG. 5. Critical magnetic fields, $\mu_0 H_{cr}$, at 2 K for $La_{1-x}Ce_xFe_{12}B_6$ series of compounds.

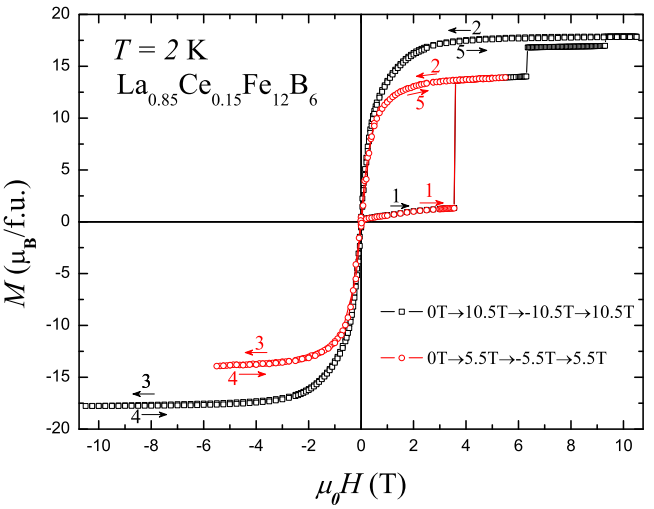

FIG. 6. Hysteresis loops of $La_{0.85}Ce_{0.15}Fe_{12}B_6$ at 2 K. The arrows indicate the field directions in which measurements have been performed.

is a large difference between pure and Ce-doped samples of $La_{1-x}Ce_xFe_{12}B_6$. In the Ce-doped compounds, the reverse leg has no steps and clearly displays the irreversible nature of the field-induced transformation; i.e., after the magnetic field is removed, the samples remain in the FM state. As regards the undoped $LaFe_{12}B_6$, the successive abrupt steps are observed not only in the virgin magnetization curve, but in the subsequent envelope as well. This implies that the forced FM state in $LaFe_{12}B_6$ loses its stability when the applied field is reduced to zero. The magnetic-field-induced FM interactions arise from the AFM state due to the sign reversal of the overall magnetic exchange parameter $\boldsymbol{J}_{ex}$. This sign reversal is likely related to the field-induced structural changes. In the parent $LaFe_{12}B_6$ compound, the FM interactions, which are induced by the application of magnetic field, can be assumed as being weak since the $LaFe_{12}B_6$ system can be transformed back to the AFM state by removal of the magnetic field. Doping with relatively small Ce atoms results in a different behavior, the field-induced ferromagnetic order being kept after removal of the magnetic field. Ce for La substitution induces both electronic and crystal lattice changes and consequently a modification of the magnetic behavior under applied field. It would be interesting to have more details on the influence of Ce on the Fe magnetic moment coupling strength to go deeper into the analysis of these Ce-induced changes.

In Fig. 5 are reported the critical magnetic fields, $\mu_0 H_{cr}$, of the step transitions at 2 K vs the Ce concentration in ZFC $La_{1-x}Ce_xFe_{12}B_6$ compounds. The transition fields decrease nearly linearly with the Ce content at a rate of -4.25 and -3.80 T/at. % Ce for the first and second magnetization step, respectively. It is remarkable that $\mu_0 H_{cr}$ is very sensitive to the Ce composition. A small change in the Ce/La ratio significantly impacts the exchange interactions. It should be noted that the unusual and unexpected staircaselike shape of the $M(\mu_0 H)$ isotherms only appears in the very-low-temperature curves, vanishing for slightly higher temperatures ($T \geqslant 8$ K).

Figure 6 displays hysteresis loops of the thermally demagnetized $La_{0.85}Ce_{0.15}Fe_{12}B_6$ compound at 2 K. The hysteresis cycles show that the forced FM state has neither magnetization remanence nor coercivity. Another noteworthy observation is that the virgin curve (path 1) lies outside the envelope curve. The magnetization curve between 0 and -10.5 T is symmetrical to the reverse leg of the first quadrant. The curve recorded when increasing the field from -10.5 to 10.5 T is superimposed on the one obtained when decreasing from 10.5 to -10.5 T. After the first application of 10.5 T, the sample thus behaves as a bulk, reversible ferromagnet. Furthermore, comparing the minor loop (recorded up to 5.5 T) to the full loop (up to 10.5 T), it is clear that during the first jump only a fraction, 77%, of the ZFC $La_{0.85}Ce_{0.15}Fe_{12}B_6$ gets transformed into a FM state.

At this point of the investigation, it is essential to check the reproducibility of the staircaselike behavior. Magnetization isotherms at 2 K were recorded on five virgin samples belonging to the same batch. For the sake of clarity, only the field-increasing branches of $M(\mu_0 H)$ are shown in Fig. 7. For all these five samples, one can point out the remarkable superimposition of the linear regimes found between 0 and 3.5 T, attesting to the good homogeneity of this set of samples. For each of them, three large jumps occur within the field range 3.5–10.5 T, and the magnetization reaches about 17.9 μ_B/f.u. under 10.5 T in all cases. The step structure is well reproducible; one just observes very small variations in the characteristic fields associated with the jumps.

In $La_{1-x}Ce_xFe_{12}B_6$, T_C is gradually shifted to higher temperatures upon increasing Ce concentration while $\mu_0 H_{cr}$ decreases with the Ce content. Both dependencies show that the initial antiferromagnetic coupling strength decreases whereas the field-induced ferromagnetic coupling becomes more easily reached upon increasing the Ce content. This may be interpreted as a progressive reduction of the stability of the AFM and a tendency to favor the ferromagnetic coupling. Hence one can suggest that the magnetic correlations in $La_{1-x}Ce_xFe_{12}B_6$ intermetallic compounds depend strongly on

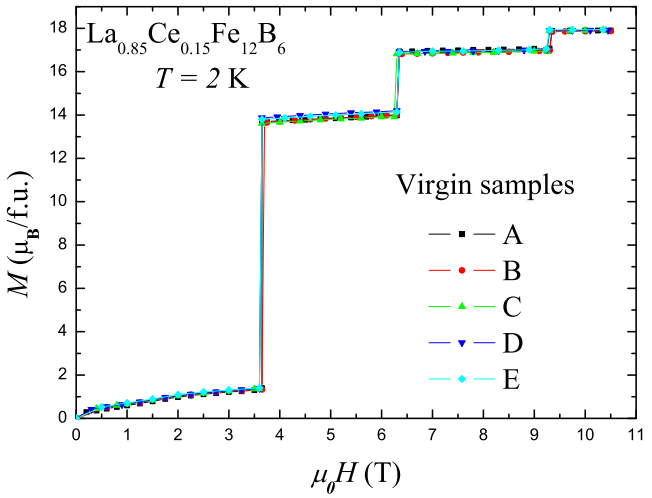

FIG. 7. First magnetization curves at 2 K in five virgin $La_{0.85}Ce_{0.15}Fe_{12}B_6$ samples coming from the same batch.

the chemical pressure and the applied magnetic field. The effect of hydrostatic pressure on the structural and magnetic properties of $LaFe_{12}B_6$ has been studied by Diop *et al.* [47]. An anisotropic shrinkage of the unit cell with a larger compression in the basal plane was observed. The application of an external pressure leads also to the progressive decrease of T_N with a moderate slope $dT_N/dP = -4.5\,K\,GPa^{-1}$. In addition a large pressure sensitivity of $\mu_0 H_{cr}$ was discovered. The critical field drastically increases upon increasing the applied pressure with an initial slope $d\mu_0 H_{cr}/dP = 24\,T\,GPa^{-1}$. In $LaFe_{12}B_6$ the application of external pressure enhances the stability of the AFM phase. In this case the effect of hydrostatic pressure is opposite to that produced by the Ce for La substitution. This indicates that the influence of Ce cannot be restricted to a simple steric effect but that electronic effect may play a role. To summarize, data presented here and reported earlier demonstrate that three quite different parameters, i.e., chemical composition, magnetic field, and external pressure, can strongly affect exchange interactions in $La_{1-x}Ce_xFe_{12}B_6$ systems.

To clarify the magnetic states at different temperatures and fields, magnetization isotherms were measured under various conditions. The initial magnetization data and the corresponding field-decreasing branches at several fixed temperatures for the $La_{0.85}Ce_{0.15}Fe_{12}B_6$ compound are presented in Figs. 8–11. Each isothermal magnetization curve starts from a ZFC state, i.e., the virgin state. Figure 8 displays the data at temperatures ranging from 2 to 9 K, Fig. 9 shows the isotherms taken between 15 and ∼33 K, Fig. 10 illustrates the cases with temperature from 35 to ∼48 K, and Fig. 11 represents isothermal magnetization measured at temperatures between 55 and 85 K. There is a distinct hysteresis between the field-increasing and field-decreasing branches of the isothermal magnetization data. Above 95 K, no field-induced phase transitions have been observed in the virgin magnetization curves in the magnetic field below our maximum attainable value of 10.5 T. Inspecting Figs. 8–11, it is obvious that the magnetization behavior is different in each of the four temperature ranges. Below 8 K, a discontinuous field-induced first-order AFM-FM metamagnetic transition occurs, as shown in Fig. 8. Three sudden jumps are detected and the corresponding critical fields decrease upon increasing temperature. Furthermore, three components in the virgin $M(\mu_0 H)$ curves are clearly seen across the AFM to FM transition in this temperature range: a sharp discontinuity followed by a plateau, before smoothly tending to saturation. The relative contribution of these three components to the magnetization value changes systematically; i.e., the metamagnetic discontinuity becomes less evident and the smooth behavior becomes more prominent, and finally dominates at $T \geqslant 8$ K.

Above 8 K, the AFM-FM transition occurring below T_N and the PM-FM transition (above T_N) exhibit a gradually increasing magnetization unlike the discontinuous behavior at very low temperature. Above 8 K and below 15 K the value of $\mu_0 H_{cr}$ decreases with temperature, while between 15 and ∼33 K the critical magnetic field becomes nearly constant. Below 15 K the critical transition field increases with lowering the temperature because thermal fluctuations of the magnetic moments and/or elasticity of the lattice in the AFM ground state are reduced, thus enhancing negative exchange interaction.

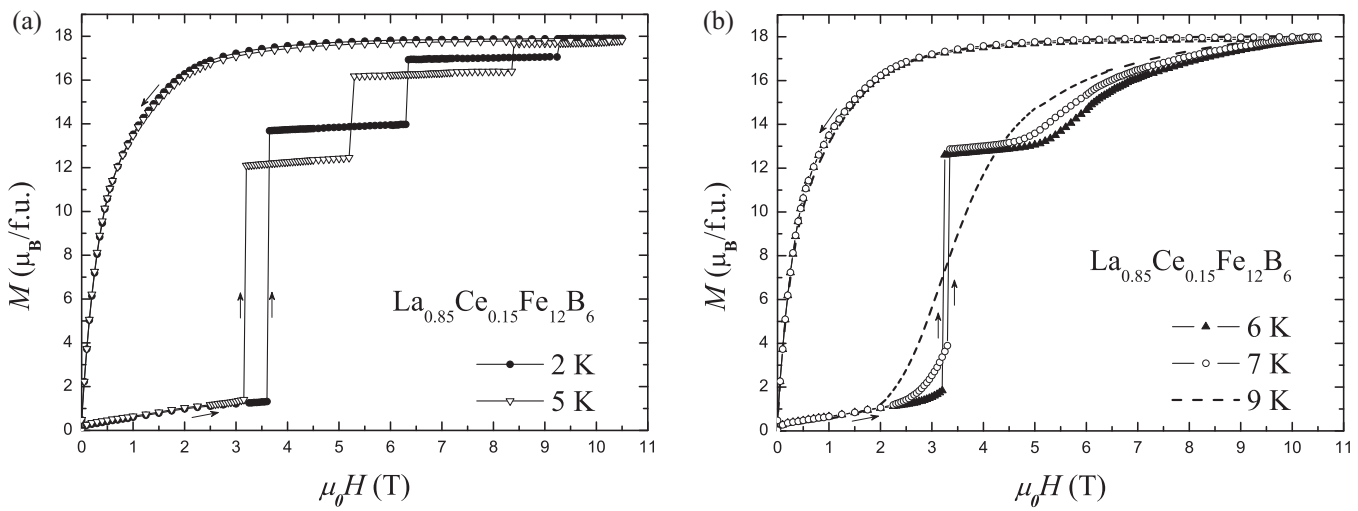

FIG. 8. Isothermal magnetization of $La_{0.85}Ce_{0.15}Fe_{12}B_6$ at (a) 2 and 5 K, and (b) 6, 7, and 9 K.

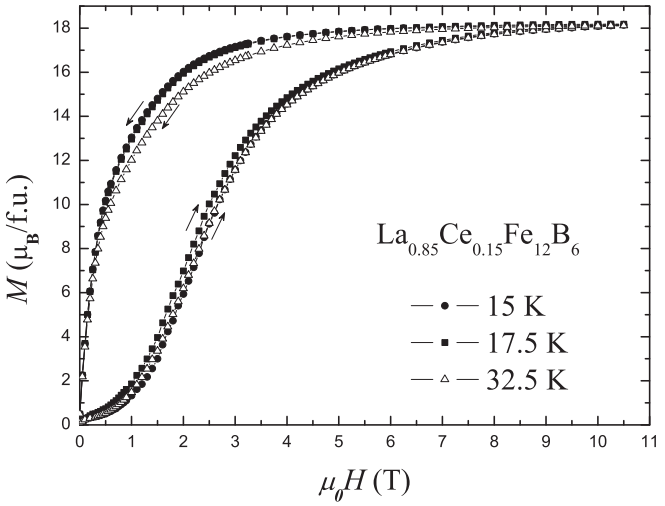

FIG. 9. Isothermal magnetization of $La_{0.85}Ce_{0.15}Fe_{12}B_6$ measured between 15 and 33 K.

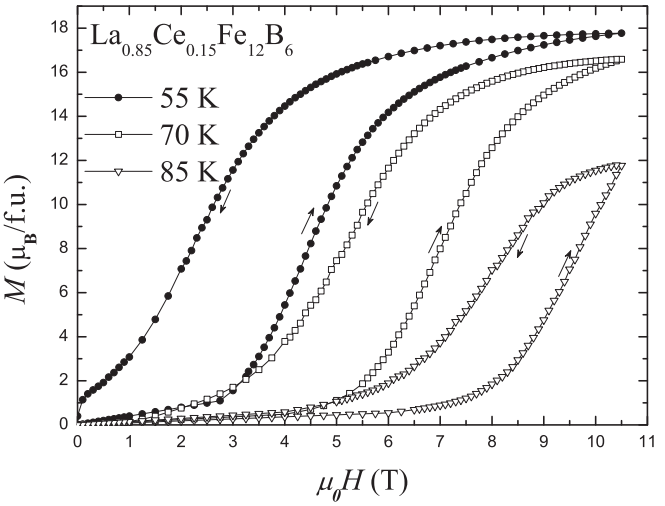

FIG. 11. Isothermal magnetization of $La_{0.85}Ce_{0.15}Fe_{12}B_6$ measured above 50 K.

Hence the increased negative exchange interaction raises both the free-energy difference between the AFM and FM states, and the critical field required to accomplish the metamagnetic phase transition [25,35].

At a temperature above 35 K, the reverse leg gradually deviates from the pure FM behavior and begins to display a metamagneticlike behavior (see the low-field portion on the field-decreasing legs of Fig. 10), which reflects a mixture of PM and FM states in the temperature range (∼35−∼55 K) upon removal of the magnetic field. Therefore, the PM-FM transformation in the temperature range of 35–55 K becomes partially reversible, as clearly seen in Fig. 12(b) during the second field increase. The critical magnetic field corresponding to the PM-FM phase transition increases with temperature, which is understandable by considering that the free-energy difference between the PM and FM states increases upon heating and the transformation from one state to another requires a higher magnetic energy to overcome the free-energy difference.

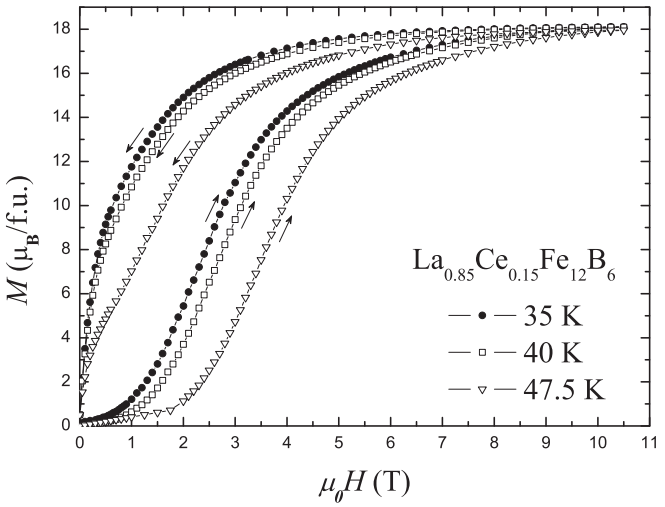

FIG. 10. Isothermal magnetization of $La_{0.85}Ce_{0.15}Fe_{12}B_6$ measured between 35 and 48 K.

D. Reversibility and irreversibility of the field-induced phase transformation

The magnetization of the ZFC $La_{0.85}Ce_{0.15}Fe_{12}B_6$, measured in the isothermal regime in the temperature range between 2 and 70 K, is reported in Fig. 12. At each temperature the applied field was cycled several times between 0 and 10.5 T. Below ∼35 K, the AFM-FM transformation is irreversible; during the second application of a magnetic field, the magnetization follows the first demagnetization path, indicating that the entire sample remains in the FM state. Once formed, the FM $La_{0.85}Ce_{0.15}Fe_{12}B_6$ phase is stable in this temperature range after removal of the magnetic field. From ∼35 to ∼55 K, the magnetization during the second application of the magnetic field shows a much more complex behavior when compared to that below 35 K. Clearly, a ferromagneticlike dependence in low magnetic field is observed and it is followed by a metamagneticlike transition. Based on this observation it is possible to conclude that between ∼35 and ∼55 K the first application of the magnetic field induces the FM state in the entire volume of the PM $La_{0.85}Ce_{0.15}Fe_{12}B_6$. When the magnetic field is reduced to zero, a fraction of the sample is converted back to a PM state. Therefore both the irreversible PM-FM and reversible PM-FM transformations exist in $La_{0.85}Ce_{0.15}Fe_{12}B_6$ from ∼35 to ∼55 K. The fraction of the sample, which undergoes the reversible PM-FM transformation, increases with temperature. At temperatures exceeding 55 K the field-induced PM-FM phase transition becomes fully reversible but with a hysteresis. Unlike the behavior observed below 55 K, where the magnetization is dependent upon the previous magnetic history, the isothermal magnetization curves are completely repeatable for each temperature above 55 K when the magnetic field is cycled. It is worth noticing that during the third and any additional application of a magnetic field between 2 and 70 K, the magnetization follows the same path as during the second field increase.

To better understand the interplay between the different magnetic states, we investigated the temperature dependence of the AFM and PM states recovered from the magnetic-field-induced FM state. For these measurements, the ZFC sample

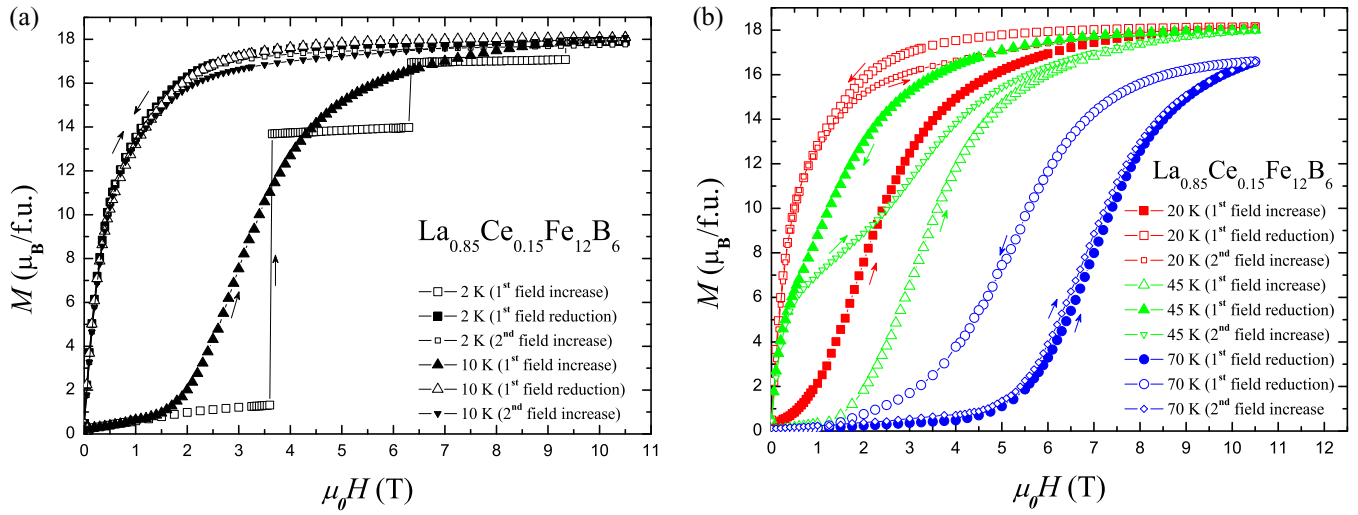

FIG. 12. Isothermal magnetization of $La_{0.85}Ce_{0.15}Fe_{12}B_6$ at (a) 2 and 10 K, and (b) 20, 45, and 70 K.

was magnetized at 2 K using a magnetic field of 10.5 T, then warmed up to the measurement temperature in zero field and $M(\mu_0 H)$ data were recorded. The amount of the residual FM phase was evaluated from the isothermal magnetization data by employing a method similar to that described by Levin *et al.* [25]. Figure 13 shows the variation of the residual FM phase in $La_{0.85}Ce_{0.15}Fe_{12}B_6$ as a function of temperature. The field-induced FM state is stable in zero magnetic field at 2 K. The premagnetized $La_{0.85}Ce_{0.15}Fe_{12}B_6$ sample remains ferromagnetic when warmed up to a temperature as high as 35 K in zero magnetic field. Below ~35 K, the magnetic-field-induced FM phase has not been thermally transformed back to the AFM state. The PM state is recovered from the field-induced FM state in a linear fashion between ~35 and ~55 K, as indicated by the solid line in Fig. 13. Therefore, the partially recovered PM state exists in the temperature range from ~35 to ~55 K together with the residual FM state in the $La_{0.85}Ce_{0.15}Fe_{12}B_6$ sample which was premagnetized at a lower temperature. Above ~55 K, the PM state is fully recovered from the field-induced FM state.

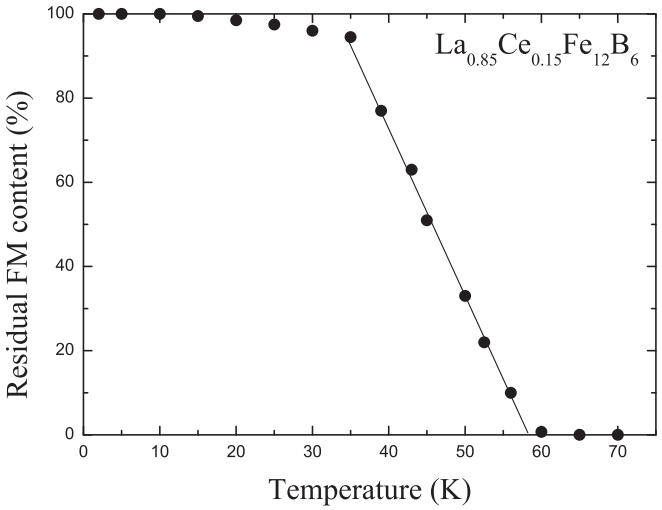

FIG. 13. Thermal evolution of the amount of the residual FM phase in the polycrystalline $La_{0.85}Ce_{0.15}Fe_{12}B_6$ sample after initial magnetization at 2 K. The solid line is a guide for the eye.

E. Influence of the magnetic field strength applied upon cooling

Since field cooling can change the relative fraction of FM and AFM phases, we have also studied the effect of the cooling field on the staircaselike transitions. For these measurements, the sample was field cooled with $\mu_0 H > 0$ T from room temperature down to the lowest desired temperature. After stabilization at the measurement temperature, the magnetic field was reduced to zero, and then isothermal $M(\mu_0 H)$ was measured up to 10.5 T and back down to zero field. Figure 14(a) presents a few isothermal magnetization curves of $La_{0.85}Ce_{0.15}Fe_{12}B_6$ measured at 2 K after different field-cooling processes (between 0 and 10 T). At 2 K, such field cooling increases the FM fraction of the sample at low fields at the expense of the AFM phase and thus results in a larger low-field magnetization. The cooling field dependence of the FM fraction is illustrated in Fig 14(b). The amount of the FM phase formed increases from 0 ($\mu_0 H = 0$ T) to ~43% ($\mu_0 H =$ 2 T), ~84% ($\mu_0 H = 4$ T), ~97% ($\mu_0 H = 6$ T), and 100% ($\mu_0 H \geqslant 6.5$ T) indicating that the extent of the AFM-FM transition is easily controlled by the magnitude of the applied magnetic field during cooling. It is clear from Fig. 14(a) that the magnetic-field values at which the avalanches spontaneously appear depend on the FM phase fraction. We note that $\mu_0 H_{cr}$ increases with the fraction of the formed ferromagnetic phase. Field cooling in a sufficiently high external applied magnetic field converts the sample into a fully ferromagnetic state, eliminating the magnetization steps. It is quite surprising that the transition fields increase after field cooling since field cooling should enhance tendencies to ferromagnetic state. Such shift of the step transitions upon increasing the cooling field was also observed in the other studied $La_{1-x}Ce_xFe_{12}B_6$ compositions. However, for the reference compound $LaFe_{12}B_6$ [39], although field cooling increases the low-field magnetization, the step transitions are shifted to lower magnetic fields contrary to what we observe for the Ce-doped $La_{1-x}Ce_xFe_{12}B_6$ pseudoternary compounds.

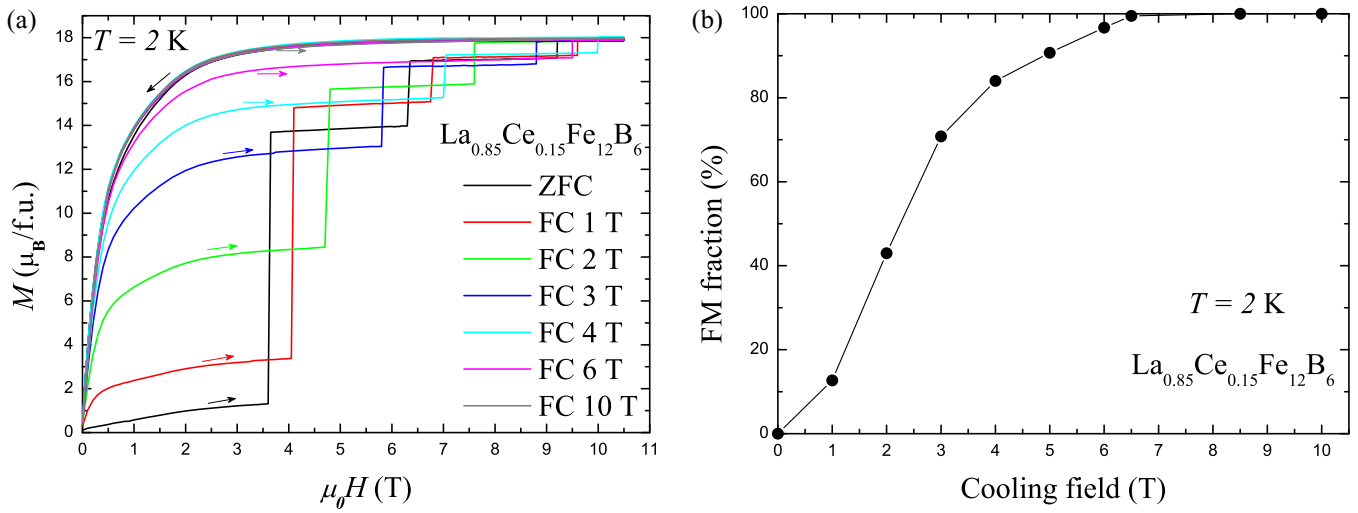

FIG. 14. (a) Isothermal magnetization of $La_{0.85}Ce_{0.15}Fe_{12}B_6$ at 2 K taken after cooling the sample in different magnetic fields from room temperature. (b) Cooling field dependence of the FM fraction.

F. Time-dependent phenomena

To further investigate more directly the dynamics of the magnetization steps, we carried out relaxation experiments at 2 K and in magnetic fields in the vicinity of the critical fields corresponding to the sharp steps observed in the isothermal $M(\mu_0 H)$ curves. Prior to these relaxation experiments, the $La_{1-x}Ce_xFe_{12}B_6$ samples were cooled in zero field from room temperature down to 2 K. After stabilization at the measurement temperature (2 K), a magnetic field is applied and the magnetization recorded as a function of time. This experimental procedure was repeated applying different magnetic fields in steps of 0.1 T. The results of relaxation measurements on $La_{0.85}Ce_{0.15}Fe_{12}B_6$ are plotted in Fig. 15. There are magnetic-field values at which giant spontaneous magnetization jumps occur when measuring as a function of time. For an applied field of 3.4 T, the magnetization of $La_{0.85}Ce_{0.15}Fe_{12}B_6$ suddenly changes from 1.35 to 13.01 μ_B/f.u. In the case of $La_{0.85}Ce_{0.15}Fe_{12}B_6$, the incubation time is found to be about 3810, 2580, and 3000 s for the first, second, and third magnetization jump, respectively. The data for the other studied compositions also reveal that the abrupt jumps in the relaxation curves can occur after a very long time. The obtained incubation times for the $La_{1-x}Ce_xFe_{12}B_6$ series of compounds are given in Table II. As can be seen in Fig. 15, the extremely sharp magnetization steps take place over a time interval smaller than the separation between two consecutive points, i.e., <30 s. The salient feature of the relaxation curves is the appearance of spontaneous magnetization jumps where both the magnetic field and the temperature are constant. We have checked the quality of the temperature stabilization over the relaxation measurements (2.00 ± 0.02 K). It must be noticed that the magnetic field is applied by a superconducting coil in the persistent mode and one can also expect the field to be very stable during the measuring time. The spontaneous character of the step transitions (in a constant field) indicates that the phenomenon is not solely driven by a change in the magnetic energy term. The singular stepwise magnetic relaxation curve (e.g., 3.4 T) is reminiscent of an explosive instability, where the magnetization displays a huge increase in a very short time [20,35].

In order to assess the deterministic or stochastic nature of these instabilities, we have checked the reproducibility of the characteristic time of the spontaneous magnetization

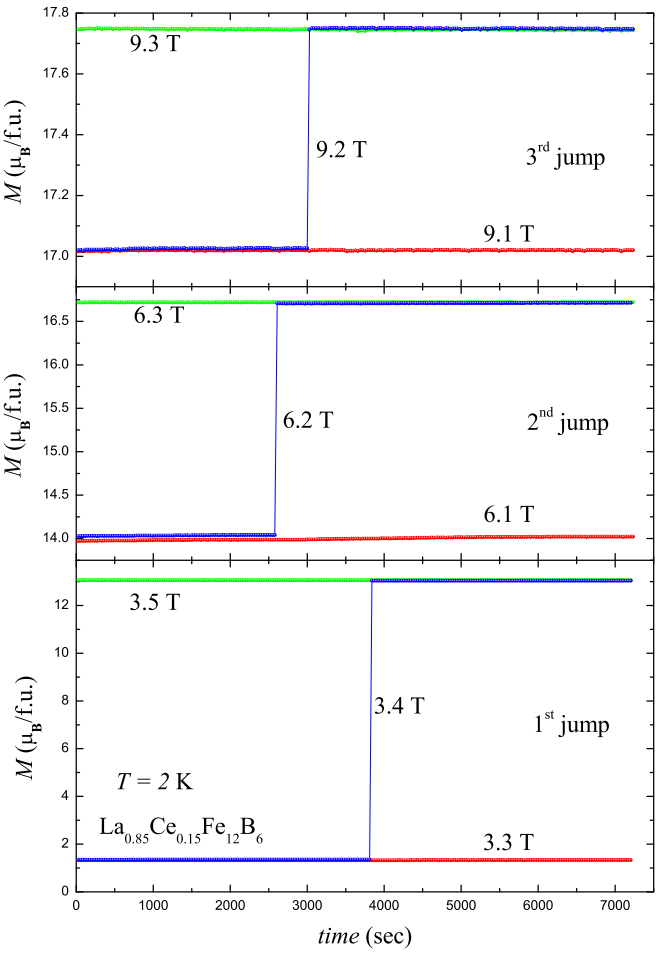

FIG. 15. Time dependence of isofield magnetization curves recorded at the indicated applied fields for $La_{0.85}Ce_{0.15}Fe_{12}B_6$ compound at 2 K.

TABLE II. Incubation (t_{inc}) and relaxation (τ) times for the $La_{1-x}Ce_xFe_{12}B_6$ series of compounds.

x	t_{inc} First jump (s)	t_{inc} Second jump (s)	t_{inc} Third jump (s)	τ (s)
0	3420	150		7500
0.05	5460	1560		7830
0.1	5550	1080		4720
0.15	3810	2580	3000	8640
0.175	4860	1300		6200

jumps. To get a direct insight into this point, we performed repeated relaxation experiments. Several $M(t)$ curves have successively been measured at 2 K, each of them starting after a ZFC protocol. Actually, the set of data indicates that the step structure is reproducible; however, a marked scatter exists about the characteristic time associated with the jump. The incubation time significantly differs from run to run. These results demonstrate that the characteristic time of the jump is not a constant characteristic of the material. For the sake of clarity, just the results of the first run are shown in Fig. 15.

Normalized magnetization M/M_0 is plotted vs time in Fig. 16. M_0 corresponds to the initial magnetization measured at $t = 0$ for each applied field. No time dependence is detected for the magnetic relaxation curve recorded in 3.5 T (i.e., above the field value at which the jump appears). On the other hand, the 3.3 T curve shows weak but sizable time dependence and it can be fitted by a simple relaxation law of the form

$$M(\mu_0 H,t) = M_0(\mu_0 H) + [M_\infty(\mu_0 H) - M_0(\mu_0 H)]\left\{1 - \exp\left[-\frac{t}{\tau(\mu_0 H)}\right]\right\}, \quad (1)$$

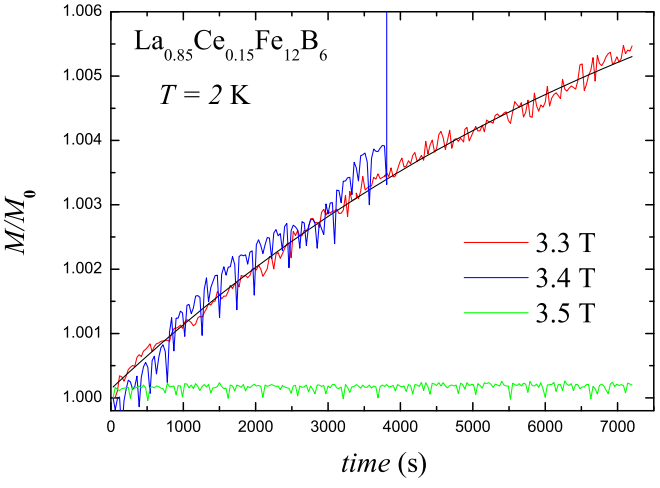

FIG. 16. Relative variation of the magnetization of $La_{0.85}Ce_{0.15}Fe_{12}B_6$ compound as a function of time (M_0 is the initial magnetization measured at $t = 0$), in magnetic fields ranging from 3.3 to 3.5 T at 2 K. The black solid line is a fitting curve for the field value of 3.3 T.

where M_∞ is the magnetization at $t = \infty$ and τ is the relaxation time. τ is related to the magnitude of the energy barrier between two metastable states [18,51]. The deduced τ values for the entire series of samples are summarized in Table II. The relaxation times τ of $La_{1-x}Ce_xFe_{12}B_6$ solid solutions vary from 4720 to 8640 s. For comparison purposes, the τ values in some manganese-based perovskites exhibiting similar features lie in the range of 5600–7100 s [20].

In view of the anomalous features seen in the data presented above, we have further investigated the magnetization dynamics by studying the influence of the magnetic-field sweep rate ($dH/dt = \dot{H}$) on the field-induced transformations. In $La_{1-x}Ce_xFe_{12}B_6$ systems, the positions of the magnetization jumps and the height of the first plateau are found to be strongly affected by the value of $\dot{H}$. The influence of the magnetic-field sweep rate on the magnetization steps is a feature that can be accounted for within a martensiticlike scenario. Indeed, for isothermal martensitic transformations, it is established that the rate of variation of the driving force (here the applied magnetic field) can affect the development of the transformation [8].

The steplike transitions observed in the $La_{1-x}Ce_xFe_{12}B_6$ series of compounds at very low temperatures are similar to those reported in many oxides [7,8,16–24]. There are some similarities in this peculiar multistep behavior with rare intermetallic compounds like Gd_5Ge_4 [8,25] and Nd_5Ge_3 [31]. These unusual features found in completely different classes of materials (oxides and intermetallics) turn out to be qualitatively consistent with the previously proposed martensiticlike scenario [8,31,33,35]. In such a scenario, the steep magnetization jumps correspond to a burstlike growth of the ferromagnetic fraction at the expense of the antiferromagnetic component, driven by the evolution of the strains at the interfaces between the two kinds of domains.

IV. CONCLUSIONS

The rhombohedral crystal structure of the $La_{1-x}Ce_xFe_{12}B_6$ compounds is preserved at least as far as $x = 0.175$. For certain magnetic-field values, the $La_{1-x}Ce_xFe_{12}B_6$ series of compounds presents a sequence of two successive magnetic transitions upon heating: an antiferromagnetic-ferromagnetic transition at low temperature followed by a ferromagnetic-paramagnetic transition. The substitution of Ce for La leads to a pronounced increase of the ferromagnetic-paramagnetic transition temperature. At finite temperatures, we have demonstrated that both AFM and PM states can be transformed to a FM state via a magnetic-field-induced first-order transition accompanied with a huge magnetic hysteresis. At low temperature the AFM-FM transition occurs via multiple ultrasharp magnetization jumps. The critical magnetic fields of the multiple step transitions were found to be extremely sensitive to Ce doping. Moreover, the magnetic relaxation exhibits a huge spontaneous step after a long incubation time when both the temperature and the magnetic field are constant. This unique and unusual stepwise relaxation effect observed in $La_{1-x}Ce_xFe_{12}B_6$ sheds light on the phenomenon of magnetization avalanches found in different classes of materials.

[1] A. K. Pathak, D. Paudyal, W. T. Jayasekara, S. Calder, A. Kreyssig, A. I. Goldman, K. A. Gschneidner, Jr., and V. K. Pecharsky, Phys. Rev. B **89**, 224411 (2014).

[2] E. Lovell, A. M. Pereira, A. D Caplin, J. Lyubina, and L. F Cohen, Adv. Energy Mater. **5**, 1401639 (2015).

[3] B. S. Shivaram, B. Dorsey, D. G. Hinks, and P. Kumar, Phys. Rev. B **89**, 161108(R) (2014).

[4] J. Liu, D. Paudyal, Y. Mudryk, J. D. Zou, K. A. Gschneidner, Jr., and V. K. Pecharsky, Phys. Rev. B **88**, 014423 (2013).

[5] J. B. Staunton, M. dos Santos Dias, J. Peace, Z. Gercsi, and K. G. Sandeman, Phys. Rev. B **87**, 060404(R) (2013).

[6] M. E. Gruner, W. Keune, B. Roldan Cuenya, C. Weis, J. Landers, S. I. Makarov, D. Klar, M. Y. Hu, E. E. Alp, J. Zhao, M. Krautz, O. Gutfleisch, and H. Wende, Phys. Rev. Lett. **114**, 057202 (2015).

[7] R. Mahendiran, A. Maignan, S. Hebert, C. Martin, M. Hervieu, B. Raveau, J. F. Mitchell, and P. Schiffer, Phys. Rev. Lett. **89**, 286602 (2002).

[8] V. Hardy, S. Majumdar, S. Crowe, M. R. Lees, D. M. Paul, L. Hervé, A. Maignan, S. Hébert, C. Martin, C. Yaicle, M. Hervieu, and B. Raveau, Phys. Rev. B **69**, 020407(R) (2004).

[9] L. M. Fisher, A. V. Kalinov, I. F. Voloshin, N. A. Babushkina, D. I. Khomskii, Y. Zhang, and T. T. M. Palstra, Phys. Rev. B **70**, 212411 (2004).

[10] S. B. Roy, P. Chaddah, V. K. Pecharsky, and K. A. Gschneidner, Jr., Acta Mater. **56**, 5895 (2008).

[11] N. V. Baranov, A. V. Proshkin, C. Czternasty, M. Meißner, A. Podlesnyak, and S. M. Podgornykh, Phys. Rev. B **79**, 184420 (2009).

[12] L. J. De Jongh and A. R. Miedema, Adv. Phys. **23**, 1 (1974).

[13] E. Stryjewski and N. Giordano, Adv. Phys. **26**, 487 (1977).

[14] V. K. Pecharsky and K. A. Gschneidner, Jr., Phys. Rev. Lett. **78**, 4494 (1997).

[15] A. Fujita, S. Fujieda, Y. Hasegawa, and K. Fukamichi, Phys. Rev. B **67**, 104416 (2003).

[16] S. Hebert, A. Maignan, V. Hardy, C. Martin, M. Hervieu, and B. Raveau, Solid State Commun. **122**, 335 (2002).

[17] A. Maignan, S. Hebert, V. Hardy, C. Martin, M. Hervieu, and B. Raveau, J. Phys.: Condens. Matter **14**, 11809 (2002).

[18] D.-q. Liao, Y. Sun, R.-f. Yang, Q.-a. Li, and Z.-h. Cheng, Phys. Rev. B **74**, 174434 (2006).

[19] V. Hardy, S. Hebert, A. Maignan, C. Martin, M. Hervieu, and B. Raveau, J. Magn. Magn. Mater. **264**, 183 (2003).

[20] V. Hardy, A. Maignan, S. Hebert, C. Yaicle, C. Martin, M. Hervieu, M. R. Lees, G. Rowlands, D. M. Paul, and B. Raveau, Phys. Rev. B **68**, 220402(R) (2003).

[21] V. Hardy, A. Maignan, S. Hebert, and C. Martin, Phys. Rev. B **67**, 024401 (2003).

[22] T. Wu and J. F. Mitchell, Phys. Rev. B **69**, 100405(R) (2004).

[23] L. Ghivelder, R. S. Freitas, M. G. das Virgens, H. Martinho, L. Granja, G. Leyva, P. Levy, and F. Parisi, Phys. Rev. B **69**, 214414 (2004).

[24] A. Banerjee, J. Sannigrahi, S. Giri, and S. Majumdar, J. Phys.: Condens. Matter **29**, 115803 (2017).

[25] E. M. Levin, K. A. Gschneidner, Jr., and V. K. Pecharsky, Phys. Rev. B **65**214427 (2002).

[26] E. M. Levin, Phys. Rev. B **80**, 144401 (2009).

[27] E. M. Levin, K. A. Gschneidner, Jr., T. A. Lograsso, D. L. Schlagel, and V. K. Pecharsky, Phys. Rev. B **69**, 144428 (2004).

[28] H. Tang, V. K. Pecharsky, K. A. Gschneidner, Jr., and A. O. Pecharsky, Phys. Rev. B **69**, 064410 (2004).

[29] Y. Mudryk, D. Paudyal, V. K. Pecharsky, K. A. Gschneidner, Jr., S. Misra, and G. J. Miller, Phys. Rev. Lett. **105**, 066401 (2010).

[30] Y. Mudryk, V. K. Pecharsky, and K. A. Gschneidner, Jr., J. Appl. Phys. **113**, 17E104 (2013).

[31] B. Maji, K. G. Suresh, and A. K. Nigam, Europhys. Lett. **91**, 37007 (2010).

[32] A. Haldar, K. G. Suresh, and A. K. Nigam, Intermetallics **18**, 1772 (2010).

[33] A. Haldar, K. G. Suresh, and A. K. Nigam, Phys. Rev. B **78**, 144429 (2008).

[34] S. B. Roy, M. K. Chattopadhyay, P. Chaddah, and A. K. Nigam, Phys. Rev. B **71**, 174413 (2005).

[35] L. V. B. Diop, O. Isnard, and J. Rodríguez-Carvajal, Phys. Rev. B **93**, 014440 (2016).

[36] S. Fujieda, K. Fukamichi, and S. Suzuki, J. Magn. Magn. Mater. **421**, 403 (2017).

[37] L. V. B. Diop, and O. Isnard, Appl. Phys. Lett. **108**, 132401 (2016).

[38] L. V. B. Diop, and O. Isnard, J. Appl. Phys. **119**, 213904 (2016).

[39] L. V. B. Diop, and O. Isnard, J. Alloys Compd. **688**, 953 (2016).

[40] K. Niihara and S. Yajima, Chem. Lett. **1**, 875 (1972).

[41] Yu. B. Kuz'ma, G. V. Chernyak, and N. F. Chaban, Dopov. Akad. Nauk. Ukr. RSR Ser. A **12**, 80 (1981).

[42] W. Jung and D. Quentmeier, Z. Kristallogr. **151**, 121 (1980).

[43] M. Mittag, M. Rosenberg, and K. H. J. Buschow, J. Magn. Magn. Mater. **82**, 109 (1989).

[44] K. H. J. Buschow, D. B. de Mooij, and H. M. van Noort, J. Less-Common Met. **125**, 135 (1986).

[45] M. Rosenberg, T. Sinnemann, M. Mittag, and K. H. J. Buschow, J. Alloys Compd. **182**, 145 (1992).

[46] Q. A. Li, C. H. de Groot, F. R. de Boer, and K. H. J. Buschow, J. Alloys Compd. **256**, 82 (1997).

[47] L. V. B. Diop, O. Isnard, Z. Arnold, J.P. Itié, J. Kastil, and J. Kamarad, Solid State Commun. **252**, 29 (2017).

[48] G. I. Miletic and Z. Blazina, J. Magn. Magn. Mater. **323**, 2340 (2011).

[49] G. I. Miletic and Z. Blazina, J. Alloys Compd. **430**, 9 (2007).

[50] A. Barlet, J. C. Genna, and P. Lethuillier, Cryogenic **31**, 801 (1991).

[51] O. Iglesias and A. Labarta, Phys. Rev. B **70**, 144401 (2004).